



## **INVERSION OF SURFACE WAVE PHASE VELOCITIES IN A SLIGHTLY ANISOTROPIC MEDIUM**

**V. Corchete<sup>1</sup> and J. Badal<sup>2</sup>**

<sup>1</sup>Department of Applied Physics, University of Almeria, Almeria, Spain.

<sup>2</sup>Department of Theoretical Physics-Geophysics, University of Zaragoza, Zaragoza, Spain

E-mail: corchete@ual.es, Fax +34 950 015477.

### **ABSTRACT**

Inversion of surface wave velocities in examples of multilayered anisotropic media is examined using an extension of the Smith-Dahlen formulation. Thus, surface wave propagation in a slightly anisotropic earth model has been found and the inversion of the azimuthal dependence of surface wave dispersion curves has been performed. The inversion scheme proposed in this paper has been verified by numerical matrix inversion with a computer programme in FORTRAN code. In two examples, hexagonal symmetry and 13 non zero canonical harmonic components, we have got results that show an excellent agreement between all phase velocities obtained for both Love and Rayleigh waves. We also perform two additional experiments with observed data, Love and Rayleigh waves phase velocities results of previous studies carry out in the Pacific (Nishimura & Forsyth, 1985, 1988, 1989). In these data test we also have a good agreement between observed and theoretical data.

### **KEYWORDS**

Surface waves, dispersion, inversion, anisotropy.

### **RESUMEN**

Se estudia la inversión de las velocidades de las ondas superficiales en ejemplos de medios anisotrópicos multiestratificados, usando una extensión de la formulación de Smith & Dahlen. Así, es estudiada la propagación de ondas superficiales en un modelo de tierra ligeramente anisotrópico y llevada a cabo la inversión de la dependencia acimutal de la dispersión de las ondas superficiales. El esquema de inversión propuesto en este artículo ha sido verificado por inversión numérica

matricial con un programa de ordenador en lenguaje FORTRAN. En dos ejemplos, simetría hexagonal y 13 componentes armónicos canónicos distintos de cero, hemos conseguido resultados que muestran un excelente acuerdo entre todas las velocidades de fase obtenidas para ambos tipos de ondas, Love & Rayleigh. También llevamos a cabo dos experimentos adicionales con datos observados: velocidades de fase de ondas Love & Rayleigh resultantes de estudios previos llevados a cabo en el Pacífico (Nishimura & Forsyth, 1985, 1988, 1989). En estas pruebas con datos también obtenemos un buen acuerdo entre datos teóricos y observados.

## **PALABRAS CLAVES**

Ondas Superficiales, dispersión, inversión, anisotropía.

## **INTRODUCTION**

Most possible constituents of the Earth are anisotropic on a small scale. Moreover, the mechanisms present today or in the past could cause alignment of this anisotropy over wide areas, particularly in the upper mantle. This anisotropy has been evidenced in recent years for the upper mantle beneath oceans, which possesses an inherent slight anisotropy. Thus, the existence of a slight anisotropy over wide areas in the Earth, probably due to a preferential alignment of olivine crystals in the upper mantle, should have an effect on the propagation of Love and Rayleigh surface waves. For this reason, the study of surface wave propagation in slightly anisotropic structures, is of importance to seismology in determining of the presence or absence of anisotropic layers within the Earth. The study of this problem, is possible on the base of a very simple hypothesis (Smith & Dahlen 1973): the azimuthal dependence of the surface wave phase velocity (Love or Rayleigh),  $c(\omega, \theta)$ , in a slightly anisotropic structure is of the form:  $c(\omega, \theta) = c(\omega) + \delta c(\omega, \theta)$ ; where  $c(\omega)$  is the isotropic phase velocity and for Love wave the anisotropy term  $\delta c(\omega, \theta)$  is of the form

$$\delta c(\omega, \theta) = \frac{1}{2G_L(\omega)} [L_1(\omega) + L_2(\omega) \cos 2\theta + L_3(\omega) \sin 2\theta + L_4(\omega) \cos 4\theta + L_5(\omega) \sin 4\theta] \quad (1)$$

and for Rayleigh wave

$$\delta(\omega, \theta) = \frac{1}{2G_R(\omega)} [R_1(\omega) + R_2(\omega) \cos 2\theta + R_3(\omega) \sin 2\theta + R_4(\omega) \cos 4\theta + R_5(\omega) \sin 4\theta] \quad (2)$$

We introduce in the above equations  $G_R(\omega)$  denoting the isotropic Rayleigh wave group velocity, and similarly  $G_L(\omega)$  denoting the isotropic Love wave group velocity. The effect of a slight anisotropy on the dispersion of surface waves is associated to the canonical harmonic components  $\gamma_{\sigma}^{lm\phi}(z)$  through the expressions (1) and (2), where the components  $\gamma_{\sigma}^{lm\phi}(z)$  are related with the elements of an arbitrary elastic tensor  $\gamma_{ijkl}(z)$  (Smith & Dahlen 1973), giving the explicit dependence of the coefficients  $L_n(\omega)$  and  $R_n(\omega)$  on the anisotropic elastic properties  $\gamma(z)$  of the half-space, are precisely the results that are required for an inversion of the data.

Our purpose with this paper is to provide an inversion scheme for the  $L_n(\omega)$  and  $R_n(\omega)$  coefficients to determine the anisotropic structure, that is, the elastic tensor  $E(z) = E_0(z) + \gamma(z)$ , where  $\gamma(z)$  is a small perturbation. The inverse problem for  $\gamma(z)$  is an incomplete problem, in the sense of that not all 21 independent canonical harmonic components  $\gamma_{\sigma}^{lm\phi}(z)$  appear explicitly, since only appear 13 independent canonical harmonic components. Nevertheless, it is a linear inverse problem and its structure is well understood. The object of this paper is precisely to explore some cases of surface wave propagation in anisotropic media, and to use the inversion theory to obtain the elastic tensor  $E(z) = E_0(z) + \gamma(z)$ . This method should be an useful tool to study the anisotropic structure of wide areas of the Earth, if we have collected sufficient high-quality dispersion data and the dominant isotropic properties of the medium are well known in advance.

## METHODS

### 2. Analytical procedure

The five coefficients  $L_n(\omega)$  for Love wave and the five coefficients  $R_n(\omega)$  corresponding to Rayleigh wave are related with the canonical

harmonic components  $\gamma_{\sigma}^{lm\phi}(z)$ . In particular,  $L_5(\omega)$  and  $R_5(\omega)$  depend explicite only on  $\gamma_S^{44s}(z)$  through the integral expressions

$$L_5(\omega) = \frac{1}{L_0} \int_0^{\infty} [-\gamma_S^{44s} \cdot W^2] dz \quad ,, \quad R_5(\omega) = \frac{1}{R_0} \int_0^{\infty} [\gamma_S^{44s} V^2] dz$$

where  $W(z)$  is some scalar function of depth corresponding to the Love wave displacement field and  $V(z)$  is an analogue function corresponding to the Rayleigh wave horizontal displacement. In a multilayered anisotropic medium,  $\gamma_S^{44s}(z)$  is constant in each layer, and then

$$L_5(\omega) = \frac{-1}{L_0} \sum_{i=1}^n \gamma_S^{44s}(z_i) \int_{z_i}^{z_{i+1}} W^2 dz \quad ,, \quad (z_1 = 0, z_2 = d_1 + z_1, \dots, z_{i+1} = d_i + z_i, \dots, z_{n+1} = \infty)$$

where  $n$  is now the number of layers of the earth model,  $d_i$  is the thickness of the  $i$ th-layer, and  $\gamma_S^{44s}(z_i)$  is the canonical harmonic component for the  $i$ th-layer. Obviously, for  $R_5(\omega)$  we write a similar relation. Note that is possible introduce a matrix formulation in the form

$$L_5(\omega_j) L_0(\omega_j) = \sum_{i=1}^n \gamma_S^{44s}(z_i) S_i(\omega_j) \quad ,, \quad S_i(\omega_j) = - \int_{z_i}^{z_{i+1}} W^2(\omega_j) dz$$

where  $\omega_j$  is a fixed angular frequency. Thus, the five coefficients  $L_n(\omega)$  for Love wave and the five ones  $R_n(\omega)$  for Rayleigh wave, are related explicitly with the canonical harmonic components  $\gamma_{\sigma}^{lm\phi}(z)$  by means of five matrices whose elements are integrals of scalar functions of depth corresponding to the surface wave displacement field for each layer. We have a matrix relation of the form:  $\mathbf{L}_5 = \mathbf{A} \mathbf{X}$ ; for the coefficient  $L_5(\omega)$ , where (using the summation convention for repeated subscripts)

$$\mathbf{L}_5 = (L_j^5) \quad (j = 1, 2, \dots, m) \quad ,, \quad L_j^5 = L_5(\omega_j) L_0(\omega_j) = A_{ji} X_i \quad ,, \quad \mathbf{X} = (X_i) \quad (i = 1, 2, \dots, n) \quad ,, \quad X_i = \gamma_S^{44s}(z_i) \quad ,, \quad \mathbf{A} = (A_{ji}) \quad ,, \quad A_{ji} = S_i(\omega_j)$$

Similarly, for the rest of coefficients  $L_n(\omega)$  and  $R_n(\omega)$  we have matrix relations of the form

$$\mathbf{L}_n = \mathbf{A} \mathbf{X} \quad , \quad \mathbf{R}_n = \mathbf{B} \mathbf{X} \quad (n = 1, 2, \dots, 5) \quad (3)$$

Equations (3) are five linear relations of the coefficients  $L_n(\omega)$  and  $R_n(\omega)$  to the canonical harmonic components  $\gamma_{\sigma}^{lm\phi}(z_i)$  that are constants for each layer. Then an inversion process to obtain  $\gamma_{\sigma}^{lm\phi}(z_i)$  from the coefficients  $L_n(\omega)$  and  $R_n(\omega)$ , can be performed by linear inversion (Aki & Richards 1980) according to the generalized inversion theory (Tarantola 1987).

## RESULTS AND DISCUSSION

### 3. Numerical procedure

The remainder of the paper discusses two examples of seismic wave propagation in earth models with slight anisotropy. In both cases the dominant isotropic properties of the medium are the same, that is, we have considered the elastic isotropic tensor  $E_{ijkl}^0(z)$  in which the Lamé constants are obtained from an isotropic earth model (Table 1).

Table 1. Isotropic earth model considered in this study for numerical computation ( $\alpha$ : compressional seismic velocity;  $\beta$ : shear velocity;  $\rho$ : mass density).

Thickness (km)	$\alpha$ (km/s)	$\beta$ (km/s)	$\rho$ (g/cm <sup>3</sup> )
10	5.80	3.40	2.70
20	6.59	3.81	2.90
80	8.135	4.670	3.324
$\infty$	9.00	5.40	3.60

Table 2. Stiffness tensor components in the matrix notation  $E_{ij}$  (first example). Units are in GPa.

$$(E_{ij}) = \begin{pmatrix} 131 & 43 & 50 & 0 & 0 & 0 \\ 43 & 131 & 50 & 0 & 0 & 0 \\ 50 & 50 & 121 & 0 & 0 & 0 \\ 0 & 0 & 0 & 40 & 0 & 0 \\ 0 & 0 & 0 & 0 & 40 & 0 \\ 0 & 0 & 0 & 0 & 0 & 44 \end{pmatrix}$$

thickness = 20 km  
density = 2.90 g/cm<sup>3</sup>  
symmetry: hexagonal

$$(E_{ij}) = \begin{pmatrix} 230 & 80 & 85 & 0 & 0 & 0 \\ 80 & 230 & 85 & 0 & 0 & 0 \\ 85 & 85 & 210 & 0 & 0 & 0 \\ 0 & 0 & 0 & 70 & 0 & 0 \\ 0 & 0 & 0 & 0 & 70 & 0 \\ 0 & 0 & 0 & 0 & 0 & 75 \end{pmatrix}$$

thickness = 80 km  
density = 3.324 g/cm<sup>3</sup>  
symmetry: hexagonal

Table 3. Stiffness tensor components in the matrix notation  $E_{ij}$  (second example). Units are in GPa.

$$(E_{ij}) = \begin{pmatrix} 131 & 43 & 50 & 0 & 0 & 0 \\ 43 & 131 & 50 & 0 & 0 & 0 \\ 50 & 50 & 121 & 0 & 0 & 0 \\ 0 & 0 & 0 & 40 & 0 & 0 \\ 0 & 0 & 0 & 0 & 40 & 0 \\ 0 & 0 & 0 & 0 & 0 & 44 \end{pmatrix}$$

thickness = 20 km  
density = 2.90 g/cm<sup>3</sup>  
symmetry: hexagonal

$$(E_{ij}) = \begin{pmatrix} 260 & 87 & 69 & 0 & 0 & 10 \\ 87 & 232 & 65 & 0 & 0 & 6 \\ 69 & 65 & 218 & 0 & 0 & 0 \\ 0 & 0 & 0 & 65 & -3 & 0 \\ 0 & 0 & 0 & -3 & 63.5 & 0 \\ 10 & 6 & 0 & 0 & 0 & 75.5 \end{pmatrix}$$

thickness = 80 km  
density = 3.324 g/cm<sup>3</sup>  
symmetry: free choice

In the first case, the Table 2 shows the elastic anisotropic tensor  $E_{ijkl}(z)$  from the usual definition of matrix  $E_{ij}$ , in which the indices  $i$  and  $j$  vary from 1 to 6 (Babuska & Cara 1991). Likewise, the Table 3 gives  $E_{ijkl}(z)$  for the second example. In both cases, we obtain first the azimuthal variation of Love and Rayleigh wave phase velocity (fundamental mode) by means of the equation  $c(\omega, \theta) = c(\omega) + \delta c(\omega, \theta)$ , where  $c(\omega)$  is computed from the elastic isotropic properties related to the values given in table 1 (Abo-Zena 1979; Kennett & Clarke 1983), and  $\delta c(\omega, \theta)$  from equations (1) and (2), in which the effect of a slight anisotropy is associated to  $\gamma_{ijkl}(z)$ . Any tensor component  $\gamma_{ijkl}(z)$  is computed by  $E_{ijkl}(z) - E_{ijkl}^0(z)$ . In a second step, we compute the inversion of

relations (3) to obtain  $\gamma_{\sigma}^{lm\phi}(z_i)$  from the coefficients  $L_n(\omega)$  and  $R_n(\omega)$  calculated before. To this end we take into account errors that usually remain in the estimation of surface wave dispersion data, such as errors in the origin time of the seismic events, digitisation or background noise; in practice, we can expect an uncertainty in  $L_n(\omega)$  and  $R_n(\omega)$  of approximately 1% in very homogeneous media. Thus, in this work we consider an uncertainty of 1% for the coefficients  $L_n(\omega)$  and  $R_n(\omega)$  in order to carry out the inversion process of relations (3) to obtain  $\gamma_{ijkl}(z)$ . In order to show that the results of first a second procedure give a good agreement between all phase velocities obtained for both Love and Rayleigh waves, the inversion scheme is tested in four examples to allow an efficient calculation procedure, which could be used to perform the inversion of azimuthal dependence of the surface wave phase velocity found in different regions of the Earth.

#### 4. Testing the inversion method

For the testing of the inversion method proposed, we shall carry out the inversion of azimuthal dependence of Love and Rayleigh wave dispersion, in two numerical examples and two examples more with observed data. In the first numerical example, we shall consider an anisotropic structure with hexagonal symmetry. In the second one, we shall consider a more general anisotropy case with 13  $\gamma_{ijkl}(z)$  non-zero stiffness tensor components. Finally, we perform two experimental data test with Love and Rayleigh waves phase velocities, obtained in previous studies for the Pacific (Nishimura & Forsyth 1985, 1988, 1989).

##### *Hexagonal symmetry*

Several studies (Nishimura & Forsyth 1989) show that realistic models are obtained by assuming transversely isotropy (hexagonal symmetry) with the axis of symmetry oriented vertically. For this reason we shall consider this kind of symmetry in the first example. With this goal in mind, we take into consideration an earth model so that the elastic isotropic tensor is obtained from the parameters given in table 1, and the elastic anisotropic tensor  $E_{ijkl}(z)$  is given in table 2. Then, we obtain the Love and Rayleigh wave phase velocity (fundamental mode) and  $\delta c(\omega, \theta)$  from equations (1) and (2), in which the effect of a slight

anisotropy is associated to  $\gamma_{ijkl}(z)$ . Finally, we compute the inversion of relations (3) to obtain  $\gamma_{\sigma}^{lm\phi}(z_i)$  from the coefficients  $L_n(\omega)$  and  $R_n(\omega)$  already calculated, by considering an uncertainty in  $L_n(\omega)$  and  $R_n(\omega)$  of approximately 1%. Results of this procedure for the perturbations of the stiffness tensor components are shown in table 4, in which we can see that it is possible to obtain  $\gamma_{ijkl}(z)$  with a small error.

*13 canonical harmonic components non zero.*

In this second example we take into consideration the same starting earth model. The elastic isotropic tensor is obtained again from the parameters listed in Table 1, but the elastic anisotropic tensor  $E_{ijkl}(z)$  is given now by Table 3. As before, we obtain in this case the azimuthal variation of Love and Rayleigh wave phase velocity (see figures 1 and 2) from equations (1) and (2). We compute the inversion of relations (3) to obtain  $\gamma_{\sigma}^{lm\phi}(z_i)$  from the coefficients  $L_n(\omega)$  and  $R_n(\omega)$  and with an uncertainty in  $L_n(\omega)$  and  $R_n(\omega)$  of approximately 1%. Results of this procedure show again that it is possible to obtain  $\gamma_{ijkl}(z)$  with a small error, also when the 13  $\gamma_{ijkl}(z)$  are non zero. The outputs in terms of Love and Rayleigh wave phase velocity depending on the azimuth are shown in figures 1 and 2.

Table 4. Perturbations of the stiffness tensor components and 1- $\sigma$  errors ( $\gamma_{ij} \pm \Delta\gamma_{ij}$ ). Units are in Gpa.

$$(\gamma_{ij}) = \begin{pmatrix} (5.1 \pm 0.4) & (1.25 \pm 0.21) & (8.25 \pm 0.19) & 0 & 0 & 0 \\ (1.25 \pm 0.21) & (5.1 \pm 0.4) & (8.25 \pm 0.19) & 0 & 0 & 0 \\ (8.25 \pm 0.19) & (8.25 \pm 0.19) & (-4.9 \pm 0.6) & 0 & 0 & 0 \\ 0 & 0 & 0 & (-2.10 \pm 0.14) & 0 & 0 \\ 0 & 0 & 0 & 0 & (-2.10 \pm 0.14) & 0 \\ 0 & 0 & 0 & 0 & 0 & (-1.90 \pm 0.15) \end{pmatrix}$$

thickness = 20 km  
density = 2.90 g/cm<sup>3</sup>  
symmetry : hexagonal



$$(\gamma_{ij}) = \begin{pmatrix} (10.0 \pm 0.6) & (5.0 \pm 0.4) & (10.0 \pm 0.3) & 0 & 0 & 0 \\ (5.0 \pm 0.4) & (10.0 \pm 0.6) & (10.0 \pm 0.3) & 0 & 0 & 0 \\ (10.0 \pm 0.3) & (10.0 \pm 0.3) & (-10 \pm 1) & 0 & 0 & 0 \\ 0 & 0 & 0 & (-2.49 \pm 0.23) & 0 & 0 \\ 0 & 0 & 0 & 0 & (-2.49 \pm 0.23) & 0 \\ 0 & 0 & 0 & 0 & 0 & (2.51 \pm 0.26) \end{pmatrix}$$

thickness = 80 km  
density = 3.324 g/cm<sup>3</sup>  
symmetry : hexagonal

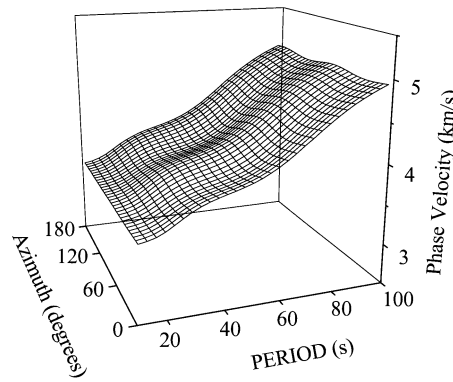


Fig. 1. Azimuthal dependence of Love wave phase velocity in a slightly anisotropic structure with elastic parameters given by Table 3.

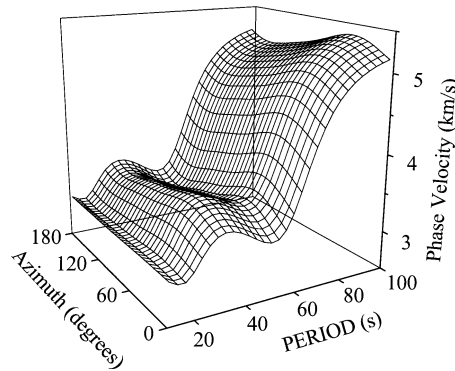
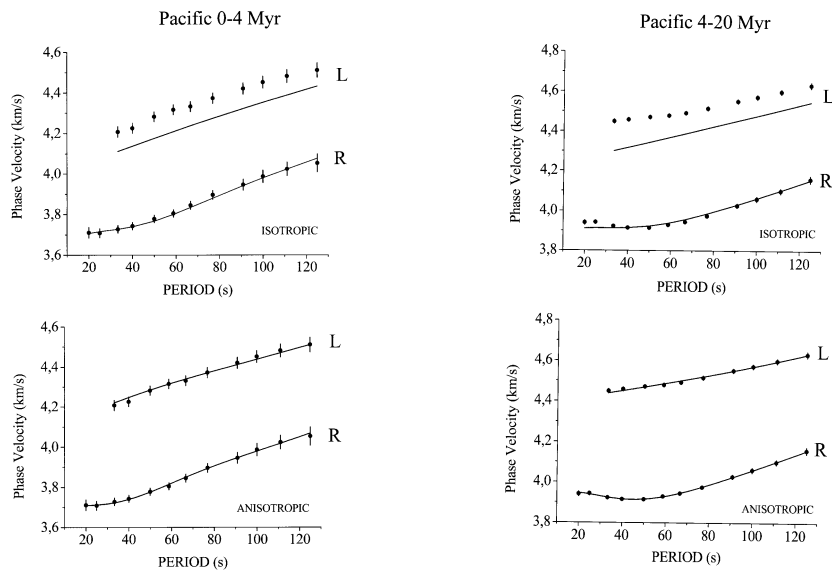


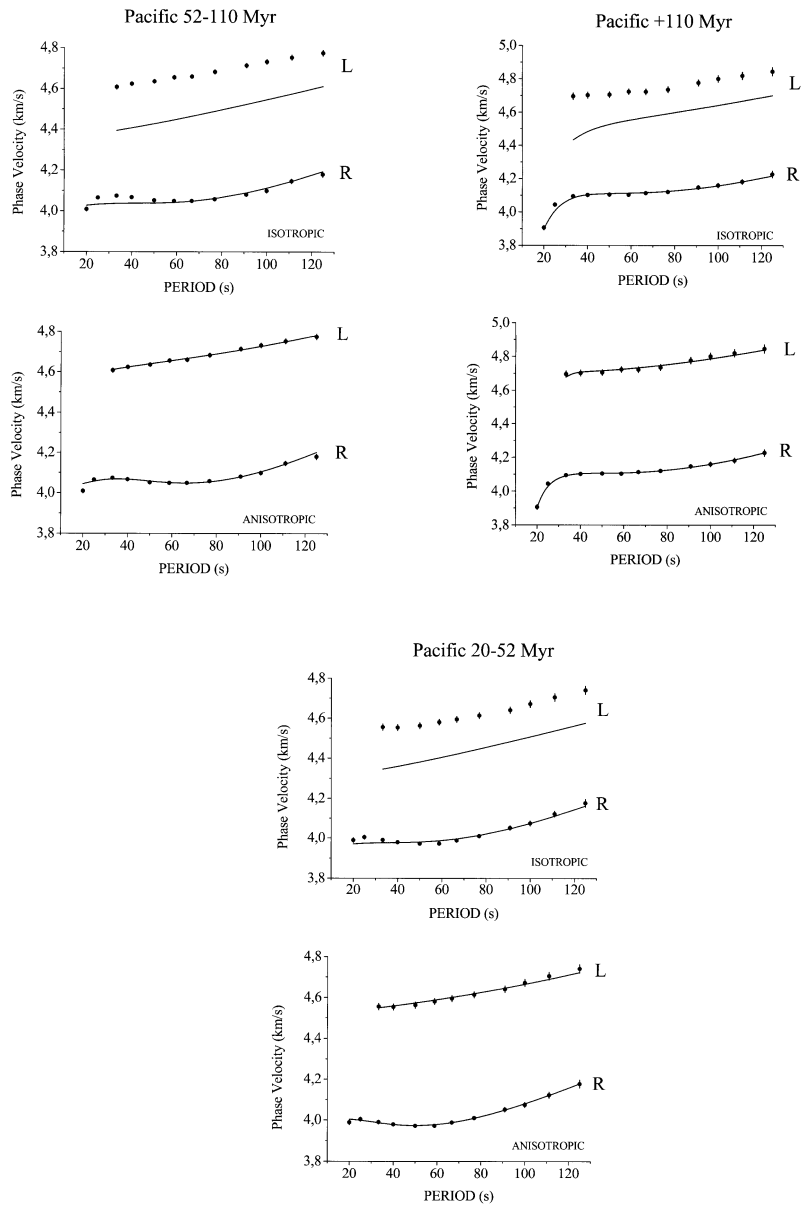
Fig. 2. Azimuthal dependence of Rayleigh wave phase velocity in a slightly anisotropic structure with elastic parameters given by Table 3.

*First experimental data test.*

As an additional reliability test of the inversion method proposed, we perform the inversion of the observed Love and Rayleigh wave dispersion, determined in previous studies for the Pacific region (Nishimura & Forsyth 1985, 1988, 1989). These dispersion curves are showed in the Figure 3, for all age regions considered in this study (0-4, 4-20, 20-52, 52-110 and 110+ Myr), with standard deviations bars at its reference periods. We shall consider an anisotropic structure with hexagonal symmetry for the inversion of these regionalized dispersion curves, because no azimuthal dependence of surface waves propagation are given in these dispersion data.

Fig. 3. Love and Rayleigh wave phase velocities used in this study (Nishimura & Forsyth 1985, 1988, 1989). For each age region we show a comparison between observed values (small circles with vertical bars denoting 1- $\sigma$  errors) and theoretical values (continuous line). Theoretical values showed in the upper part are predicted by forward modeling of the starting isotropic models (Table 5), and the other ones showed in the lower part are predicted by the final anisotropic model obtained by inversion (Table 6).





Previous to inversion process, we propose a starting isotropic earth model, for each region considered, as listed in Table 5. In Figure 3 we observe a good agreement between theoretical Rayleigh wave dispersion curves (obtained by forward modelling of the isotropic models listed in Table 5) and the corresponding observed curves, for all regions. Nevertheless, the Love wave theoretical dispersion curves

(Fig. 3) are in clear discrepancy with the respective observed curves. This fact is well known in regions of the Earth, like Pacific, in which anisotropy is present. This fact is called discrepancy Love-Rayleigh and it is a consequence of anisotropic properties of mantle materials. Then, Love and Rayleigh wave dispersion curves are not compatible with a unique isotropic model and it is necessary to consider an anisotropic model. For that reason, we perform here an anisotropic inversion.

Table 5. Starting isotropic earth models proposed for each region considered in this study ( $\alpha$ : compressional seismic velocity;  $\beta$ : shear velocity;  $\rho$ : mass density). These regions have been obtained by a regionalization scheme based on the seafloor age (Nishimura & Forsyth 1985, 1988, 1989), as result of this procedure we have five age regions: 0-4, 4-20, 20-52, 52-110 and 110+ Myr.

AGE REGION 0-4 Myr

Layer (n°)	Thickness (km)	$\alpha$ (km/s)	$\beta$ (km/s)	$\rho$ (g/cm <sup>3</sup> )
1	15	6.80	3.90	2.90
2	130	7.15	4.07	2.95
3	200	7.75	4.50	3.35
4	50	8.90	4.68	3.52
5	50	9.15	4.85	3.65
6	50	9.40	5.05	3.80
7	50	9.68	5.19	3.89
8	50	9.94	5.40	3.99
9	50	10.30	5.64	4.12
10	$\infty$	10.79	5.95	4.32

AGE REGION 4-20 Myr

Layer (n°)	Thickness (km)	$\alpha$ (km/s)	$\beta$ (km/s)	$\rho$ (g/cm <sup>3</sup> )
1	5	6.80	3.90	2.90
2	90	7.60	4.28	3.20
3	50	7.25	4.18	3.10
4	50	8.00	4.38	3.35
5	100	8.70	4.60	3.50
6	50	8.60	4.59	3.50
7	50	8.84	4.72	3.56
8	50	9.14	4.86	3.67
9	50	9.34	5.04	3.75
10	50	9.68	5.19	3.89
11	50	9.94	5.39	3.99
12	50	10.30	5.64	4.12
13	$\infty$	10.79	5.95	4.32

AGE REGION 20-52 Myr

Layer (n°)	Thickness (km)	$\alpha$ (km/s)	$\beta$ (km/s)	$\rho$ (g/cm <sup>3</sup> )
1	5	6.80	3.90	2.90
2	90	7.80	4.34	3.35
3	50	7.80	4.30	3.35
4	50	7.70	4.25	3.35
5	50	8.10	4.45	3.35
6	100	8.93	4.75	3.58
7	100	9.14	4.87	3.67
8	50	9.34	5.04	3.75
9	50	9.68	5.19	3.89
10	50	9.94	5.39	3.99
11	50	10.30	5.64	4.12
12	$\infty$	10.79	5.95	4.32

AGE REGION 52-110 Myr

Layer (n°)	Thickness (km)	$\alpha$ (km/s)	$\beta$ (km/s)	$\rho$ (g/cm <sup>3</sup> )
1	5	6.80	3.90	2.90
2	140	8.08	4.40	3.35
3	50	7.60	4.20	3.35
4	50	8.10	4.45	3.35
5	100	8.93	4.75	3.58
6	100	9.14	4.87	3.67
7	50	9.34	5.04	3.75
8	50	9.68	5.19	3.89
9	50	9.94	5.39	3.99
10	50	10.30	5.64	4.12
11	$\infty$	10.79	5.95	4.32

AGE REGION 110+ Myr

Layer (n°)	Thickness (km)	$\alpha$ (km/s)	$\beta$ (km/s)	$\rho$ (g/cm <sup>3</sup> )
1	20	5.60	3.30	2.65
2	75	8.70	4.73	3.45
3	150	8.20	4.50	3.35
4	100	8.60	4.55	3.50
5	100	9.18	4.90	3.70
6	50	9.34	5.04	3.75
7	50	9.68	5.19	3.89
8	50	9.94	5.39	3.99
9	50	10.30	5.64	4.12
10	$\infty$	10.79	5.95	4.32

This inversion process is the same to the above described (hexagonal symmetry epigraph), but now the effect of a slight anisotropy is associated (for each age region) to the second elastic layer of the Earth model. Thus, the stiffness tensor perturbations ( $\gamma_{ijkl}(z)$ ) obtained by such inversion scheme are listed in Table 6.

Table 6. Perturbations of the stiffness tensor components and 1- $\sigma$  errors ( $\gamma_{ij} \pm \Delta\gamma_{ij}$ ), for each age region considered. Units are in Gpa.

<p>AGE REGION 0-4 Myr</p> $(\gamma_{ij}) = \begin{pmatrix} (-17 \pm 11) & (-22 \pm 6) & (-3 \pm 5) & 0 & 0 & 0 \\ (-22 \pm 6) & (-17 \pm 11) & (-3 \pm 5) & 0 & 0 & 0 \\ (-3 \pm 5) & (-3 \pm 5) & (6 \pm 19) & 0 & 0 & 0 \\ 0 & 0 & 0 & (10 \pm 4) & 0 & 0 \\ 0 & 0 & 0 & 0 & (10 \pm 4) & 0 \\ 0 & 0 & 0 & 0 & 0 & (3 \pm 5) \end{pmatrix}$ <p>layer = 2 thickness = 130 km density = 2.95 g/cm<sup>3</sup> symmetry: hexagonal</p>	<p>AGE REGION 4-20 Myr</p> $(\gamma_{ij}) = \begin{pmatrix} (-18 \pm 6) & (-29 \pm 6) & (9 \pm 6) & 0 & 0 & 0 \\ (-29 \pm 6) & (-18 \pm 6) & (9 \pm 6) & 0 & 0 & 0 \\ (9 \pm 6) & (9 \pm 6) & (38 \pm 12) & 0 & 0 & 0 \\ 0 & 0 & 0 & (13 \pm 4) & 0 & 0 \\ 0 & 0 & 0 & 0 & (13 \pm 4) & 0 \\ 0 & 0 & 0 & 0 & 0 & (6 \pm 3) \end{pmatrix}$ <p>layer = 2 thickness = 90 km density = 3.20 g/cm<sup>3</sup> symmetry: hexagonal</p>
<p>AGE REGION 20-52 Myr</p> $(\gamma_{ij}) = \begin{pmatrix} (-35 \pm 8) & (-55 \pm 9) & (-4 \pm 10) & 0 & 0 & 0 \\ (-55 \pm 9) & (-35 \pm 8) & (-4 \pm 10) & 0 & 0 & 0 \\ (-4 \pm 10) & (-4 \pm 10) & (19 \pm 12) & 0 & 0 & 0 \\ 0 & 0 & 0 & (22 \pm 6) & 0 & 0 \\ 0 & 0 & 0 & 0 & (22 \pm 6) & 0 \\ 0 & 0 & 0 & 0 & 0 & (10 \pm 5) \end{pmatrix}$ <p>layer = 2 thickness = 90 km density = 3.35 g/cm<sup>3</sup> symmetry: hexagonal</p>	<p>AGE REGION 52-110 Myr</p> $(\gamma_{ij}) = \begin{pmatrix} (13 \pm 4) & (-4 \pm 3) & (25 \pm 3) & 0 & 0 & 0 \\ (-4 \pm 3) & (13 \pm 4) & (25 \pm 3) & 0 & 0 & 0 \\ (25 \pm 3) & (25 \pm 3) & (67 \pm 6) & 0 & 0 & 0 \\ 0 & 0 & 0 & (-6 \pm 2) & 0 & 0 \\ 0 & 0 & 0 & 0 & (-6 \pm 2) & 0 \\ 0 & 0 & 0 & 0 & 0 & (9 \pm 2) \end{pmatrix}$ <p>layer = 2 thickness = 140 km density = 3.35 g/cm<sup>3</sup> symmetry: hexagonal</p>
<p>AGE REGION 110+ Myr</p> $(\gamma_{ij}) = \begin{pmatrix} (3 \pm 7) & (-25 \pm 7) & (8 \pm 7) & 0 & 0 & 0 \\ (-25 \pm 7) & (3 \pm 7) & (8 \pm 7) & 0 & 0 & 0 \\ (8 \pm 7) & (8 \pm 7) & (20 \pm 8) & 0 & 0 & 0 \\ 0 & 0 & 0 & (-1 \pm 4) & 0 & 0 \\ 0 & 0 & 0 & 0 & (-1 \pm 4) & 0 \\ 0 & 0 & 0 & 0 & 0 & (14 \pm 4) \end{pmatrix}$ <p>layer = 2 thickness = 75 km density = 3.45 g/cm<sup>3</sup> symmetry: hexagonal</p>	

Table 7. Comparison of the  $\beta_v$  parameter obtained by Nishimura & Forsyth (1989) and that of this study.

AGE REGION (Myr)	Depth Range (km)	$\beta_v^*$ (km/s)	$\beta_v^+$ (km/s)
0 – 4	15 – 145	$4.472 \pm 0.152$	4.02 – 4.43
4 – 20	5 – 95	$4.743 \pm 0.132$	4.13 – 4.58
20 – 52	5 – 95	$5.040 \pm 0.178$	4.21 – 4.61
52 – 110	5 – 145	$4.192 \pm 0.071$	4.20 – 4.63
110 +	20 – 95	$4.699 \pm 0.123$	4.43 – 4.63

(\* This study)

(+ Nishimura & Forsyth 1989)

When we take to account an anisotropic model, we obtain a good agreement in both Love and Rayleigh theoretical dispersion curves and the respective observed curves (Fig. 3). This fact confirms that the final anisotropic model obtained is a valid Earth model, for each region considered. The final anisotropic model obtained for each age region is also in agreement with the another one obtained by Nishimura & Forsyth (1989), as it can see in Table 7. We compare our  $\beta_v$  parameter with the corresponding parameter calculated by Nishimura & Forsyth, because the resolving kernels obtained by these authors clearly demonstrate that the dominant parameter in their inversion scheme is  $\beta_v$ . Moreover, the  $\beta_v$  parameter is the most resolvable parameter computed by these authors, as it is showed by the resolving kernels of the inversion process follow by themselves.

#### *Second experimental data test.*

In this second data test, we take to account the azimuthal variation of the Rayleigh wave dispersion joint to Love wave dispersion (Nishimura & Forsyth 1989) for determine an anisotropic model which satisfy these dispersion data jointly. As in the previous data test, we propose a starting isotropic earth model, for each region considered, as listed in Table 8. In Figure 4 we observe a good agreement between theoretical Rayleigh wave dispersion curves (obtained by forward modelling of the isotropic models listed in Table 8) and the corresponding observed

curves, for both regions. Like the previous data test, the Love wave observed dispersion curves can not satisfy by an isotropic model (Fig. 4). Now, we perform an anisotropic inversion of azimuthal variation of the Rayleigh wave dispersion joint to Love wave dispersion, for each region considered, with 13 canonical harmonic components non-zero obtaining, as a result of this computation for each region, the stiffness tensor perturbations ( $\gamma_{ijkl}(z)$ ) listed in Table 9. We observe again a good agreement in both Love and Rayleigh theoretical dispersion curves and the respective observed curves (Fig. 4).

Table 8. Starting isotropic earth models proposed for the age regions: 0-80 and 80+ Myr ( $\alpha$ : compressional seismic velocity;  $\beta$ : shear velocity;  $\rho$ : mass density).

AGE REGION 0-80 Myr				
Layer (n°)	Thickness (km)	$\alpha$ (km/s)	$\beta$ (km/s)	$\rho$ (g/cm <sup>3</sup> )
1	5	6.80	3.90	2.90
2	90	7.65	4.22	3.30
3	100	7.60	4.20	3.30
4	150	8.75	4.65	3.50
5	50	8.84	4.72	3.56
6	50	9.14	4.86	3.67
7	50	9.34	5.04	3.75
8	50	9.68	5.19	3.89
9	50	9.94	5.39	3.99
10	50	10.30	5.64	4.12
11	$\infty$	10.79	5.95	4.32

AGE REGION 0-80 Myr				
Layer (n°)	Thickness (km)	$\alpha$ (km/s)	$\beta$ (km/s)	$\rho$ (g/cm <sup>3</sup> )
1	20	5.60	3.30	2.65
2	75	8.70	4.73	3.45
3	150	8.20	4.50	3.35
4	100	8.60	4.55	3.50
5	100	9.18	4.90	3.70
6	50	9.34	5.04	3.75
7	50	9.68	5.19	3.89
8	50	9.94	5.39	3.99
9	50	10.30	5.64	4.12
10	$\infty$	10.79	5.95	4.32



Table 9. Perturbations of the stiffness tensor components and 1- $\sigma$  errors ( $\gamma_{ij} \pm \Delta\gamma_{ij}$ ) for both age regions: 0-80 and 80+ Myr. Units are in Gpa.

AGE REGION 0-80 Myr	AGE REGION 80+ Myr
$(\gamma_{ij}) = \begin{pmatrix} (-68 \pm 11) & (-80 \pm 12) & (-20 \pm 13) & 0 & 0 & (-1.0 \pm 0.4) \\ (-80 \pm 12) & (-65 \pm 11) & (-19 \pm 13) & 0 & 0 & (-1.0 \pm 0.4) \\ (-20 \pm 13) & (-19 \pm 13) & (2 \pm 19) & 0 & 0 & (-0.8 \pm 0.8) \\ 0 & 0 & 0 & (40 \pm 8) & (1.1 \pm 0.6) & 0 \\ 0 & 0 & 0 & (1.1 \pm 0.6) & (42 \pm 8) & 0 \\ (-1.0 \pm 0.4) & (-1.0 \pm 0.4) & (-0.8 \pm 0.8) & 0 & 0 & (7 \pm 7) \end{pmatrix}$	$(\gamma_{ij}) = \begin{pmatrix} (7 \pm 7) & (-25 \pm 7) & (9 \pm 7) & 0 & 0 & (1.1 \pm 0.3) \\ (-25 \pm 7) & (0 \pm 7) & (7 \pm 7) & 0 & 0 & (1.1 \pm 0.3) \\ (9 \pm 7) & (7 \pm 7) & (20 \pm 8) & 0 & 0 & (1.1 \pm 0.5) \\ 0 & 0 & 0 & (1 \pm 4) & (-1.0 \pm 0.3) & 0 \\ 0 & 0 & 0 & (-1.0 \pm 0.3) & (-3 \pm 4) & 0 \\ (1.1 \pm 0.3) & (1.1 \pm 0.3) & (1.1 \pm 0.5) & 0 & 0 & (14 \pm 4) \end{pmatrix}$
layer = 2 thickness = 90 km density = 3.30 g/cm <sup>3</sup>	layer = 2 thickness = 75 km density = 3.45 g/cm <sup>3</sup>

Fig. 4. Love & Rayleigh wave phase velocities for the Pacific age regions: 0-80 and 80+ Myr (Nishimura & Forsyth 1985, 1988 and 1989). For each age region we show a comparison between observed values (small circles with vertical bars denoting 1- $\sigma$  errors) and theoretical values (continuous line). Theoretical values showed in the upper part are predicted by forward modeling of the starting isotropic models, and the other ones showed in the lower part are predicted by the final anisotropic model.

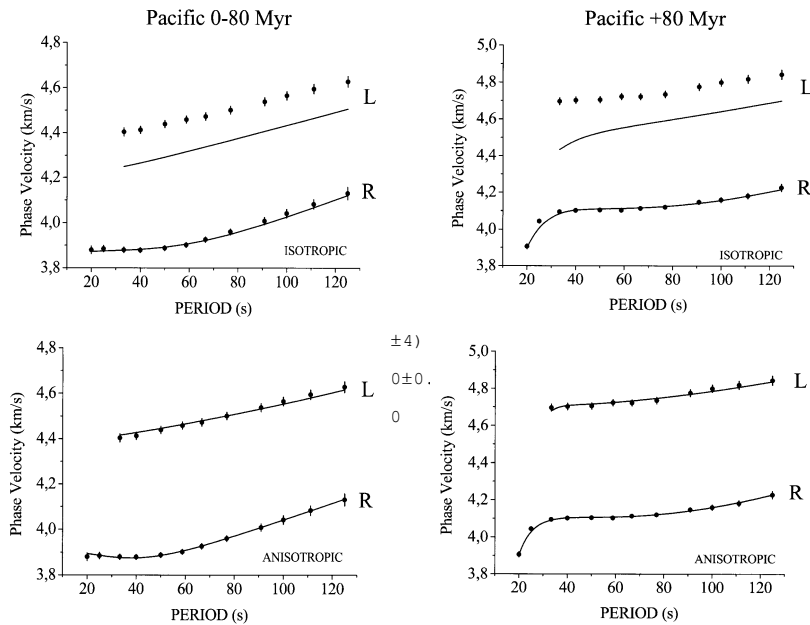
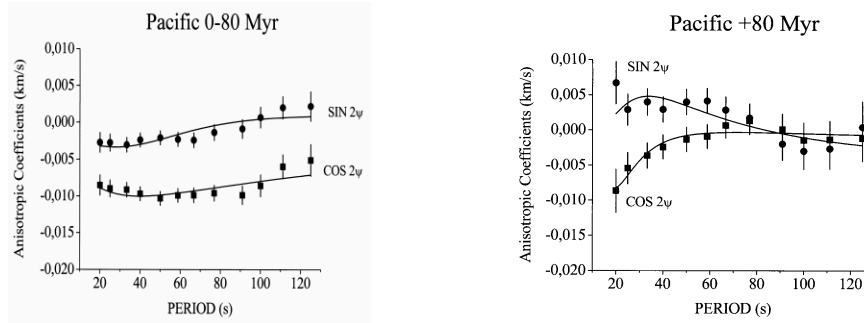


Fig. 5. Rayleigh wave azimuthal anisotropy coefficients ( $\sin 2\psi$  and  $\cos 2\psi$ ) corresponding to 0-80 and 80+ Myr age regions of the Pacific (Nishimura & Forsyth 1989), are plotted with circles and squares respectively, vertical bars denote 1- $\sigma$  errors. Theoretical values of the azimuthal anisotropy coefficients (continuous line) are predicted by the final anisotropic models.



In the other hand, we also observe that the Rayleigh wave azimuthal anisotropy coefficients are also satisfies by the anisotropic models obtained for each region (Fig. 5).

## CONCLUSIONS

Starting from the existence of a slightly anisotropy over wide areas in the Earth, the problem of the surface wave propagation in slightly anisotropic structures is re-visited from the Smith & Dahlen's hypothesis. This problem is posed as a linear inversion one and the inversion scheme proposed is performed by numerical matrix inversion. On this base, both forward and inverse modelling may be carried out, and in particular we can characterise a medium with slight anisotropy by the non zero stiffness tensor components computed from the azimuthal dependence of the surface wave velocity dispersion. The corresponding numerical procedure is indeed easy to be implemented. Four examples concerning to different anisotropic structures show the efficiency of our inversion scheme, which could be used to perform anisotropic inversion of surface wave velocity in the practice and to determine the anisotropic characteristics of some regions of the Earth. Much more realistic earth models could so be obtained.

## **ACKNOWLEDGEMENTS**

Helpful comments and suggestions from anonymous referees are gratefully acknowledged. This research was partially supported by the Dirección General de Enseñanza Superior (DGES): projects PB96-0139-C04-01-04 and by the Dirección General de Investigación, Ministerio de Ciencia y Tecnología, Spain: projects REN2000-1740-C05-03-04.

## **REFERENCES**

- Abo-Zena, A. 1979. Dispersion function computations for unlimited frequency values, *Geophys. J. R. astr. Soc.*, 58, 91-105.
- Aki, K. & P.G. Richards. 1980. *Quantitative Seismology. Theory and Methods*, Freeman, San Francisco.
- Babuska, V. & M. Cara. 1991. *Seismic Anisotropy in the Earth*, Kluwer Academic Publishers, Dordrecht, The Netherlands.
- Kennett, B. L. N. & T. J. Clarke. 1983. Rapid calculation of surface wave dispersion, *Geophys. J. R. astr. Soc.*, 72, 619-631.
- Nishimura, C. E. & D. W. Forsyth. 1985. Anomalous Love-wave phase velocities in the Pacific: sequential pure-path and spherical harmonic inversion, *Geophys. J. R. Astr. Soc.*, 81, 389-407.
- Nishimura, C. E. & D. W. Forsyth. 1988. Rayleigh wave phase velocities in the Pacific with implications for azimuthal anisotropy and lateral heterogeneities, *Geophys. J. R. Astr. Soc.*, 94, 479-501.
- Nishimura, C. E. & D. W. Forsyth. 1989 The anisotropic structure of the upper mantle in the Pacific, *Geophys. J. Int.*, 96, 203-229.
- Smith, L. M. & F. A. Dahlen. 1973. The Azimuthal Dependence of Love Wave Propagation in a Slightly Anisotropic Medium, *J. Geophys. Res.*, 78, 3321-3333.
- Tarantola, A. 1987. *Inverse Problem Theory. Methods for Data Fitting and Model Parameter Estimation*, Elsevier, Amsterdam.

*Recibido septiembre de 2003, aceptado enero de 2004.*